COHERENT NOISE REMOVAL IN SEISMIC DATA WITH REDUNDANT MULTISCALE DIRECTIONAL FILTERS

Sergi Ventosa, Hérald Rabeson, and Laurent Duval

IFP Energies nouvelles
1 et 4 avenue de Bois-Préau, 92852 Rueil-Malmaison Cedex, France
{sergi.ventosa,herald.rabeson,laurent.duval}@ifpen.fr

ABSTRACT

Directional filters are commonly used tools in modern seismic data processing to address coherent signals, depending on their apparent slowness or slope. This operation enhances the characterization of the great variety of signals present in a seismic dataset that enables a better characterization of the subsurface structure. This paper compares two complementary local adaptive multiscale directional filters: a directional filter bank based on dual-tree M-band wavelets and a novel local slant stack transform (LSST) based filter in the time-scale domain. Their differences reside in redundancy levels and slope (directional) resolution. A structural similarity index measure has been employed to objectively compare both approaches on a real seismic dataset example.

1. INTRODUCTION AND MOTIVATIONS

Understanding in geophysics is achieved thanks to seismic wave fields, recorded by arrays of sensors, as responses to artificial energy sources producing impulsive events. Each signal recorded by a sensor is a seismogram or seismic trace, sampled in time-domain. Side by side alignment of vertical 1D traces along spatial sensor location produces 2D time-offset images (seismic sections). These sections could be described as band-pass images in the vertical time direction (between 5 and 80 Hz typically), with high lateral (along offsets) semblance.

The complexity of seismic data has contributed to the development of several efficient signal processing tools such as wavelet transforms [10] or spike deconvolution. While 1D processing of seismic traces is relatively common in geophysics, their assemblage into seismic sections, as represented in Fig. 1, opens access to more involved two-dimensional processing tools. Yet, differences between traditional images and seismic sections foster the quest for specific adaptations or genuine developments. We refer to [5], freely available, for a combination of signal analysis and seismic processing topics.

The two features most commonly used to detect, separate and characterize signals seismic sections convey, are: (1) similarity along signal trajectory, and (2) velocity/slowness vector of the seismic waves at the receiver. When the seismic trace density is high in the offset axis, the high similarity enables the design of a great variety of filters depending on the signal slope, to increase the signal-to-noise and the signal-to-interference ratios.

The modern signal processing tools used in this field root in the classical plane-wave decomposition techniques. We can classify these classical techniques in broad categories: (1) pie-slice f-k (frequency-wavenumber) filters

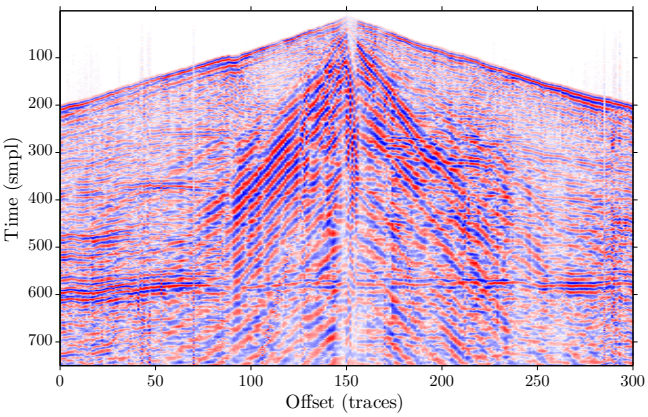

Figure 1: Original noisy data in a seismic section.

[24] based on the 2D Fourier transform; (2) τ-p (intercept-time, slope/slowness) transform, also called Radon or slant-stack transform [20, 24]; (3) p-f (slowness-frequency) filters [11, 6]; and (4) filters based on eigenvalue decompositions [22]. Note that, except the last one, all these techniques are closely related; the f-k and τ-p filters by the projection slice theorem [8], and the p-f and τ-p transforms by the Fourier transform.

These techniques are frequently adapted to be used in a local fashion to follow the slowness, amplitude and waveform variations that seismic waves usually exhibit at the cost of losing slowness resolution. The main features that distinguish the different approaches available are: the redundancy factor and the slowness/directional resolution. Multiscale geometric transforms (see [14] for a comprehensive overview) used for image processing are usually designed with reduced redundancy but mid-low slowness resolution; while continuous approaches, such as local slant-stack transform (LSST) [12, 2] or combinations between Radon and wavelet transforms [16, 18, 15], yield mid-high slowness resolution and high redundancy. Common applications on seismic signals processing are noise filtering [13] and migration operations [7].

The application under consideration focuses on the coherent noise (interferent signals) removal. This noise is caused by peculiar wave propagation and arises as structured signals in seismic sections, hampering subsequent geophysical data processing and interpretation with high amplitude directional band-pass stripes. This work investigates its removal with two breeds of selective multiscale directional decompositions: (1) a time-scale LSST, highly redundant but with a high slowness resolution and (2) a directional mul-

tiscale wavelet transform based on dual-tree M-band filterbanks with a two-fold redundancy but with a low slowness resolution. This comparison further allows to enlighten some similarities between traditional and geophysical data processing, that deserve further investigation, for the benefit of both.

The paper is organized as follows: Section 2 describes the time-scale LSST filters. Section 3 briefly recalls the principles behind the M-band dual-tree wavelets. Comparisons between the two methods are drawn in Section 4 on a real seismic dataset, followed by conclusive comments.

2. LOCAL ADAPTIVE SLANT STACK FILTERS IN THE TIME-SCALE DOMAIN

Broadly, an improvement of the accuracy of seismic signal waveform estimators in the LSST domain implies an increment of the number of samples used along the time or the offset axis. However, the instantaneous slowness variations of the seismic signals and, to a lesser extent, their amplitude variations, extremely limit the number of samples allowed along the offset axis. Moreover, we can not perform any substantial smoothing in the time axis; even though the instantaneous slowness of coherent signals are slowly varying in time, the seismic waveform is measured from its instantaneous amplitude, which varies fast.

The direct use of the instantaneous amplitude in the waveform estimation entails the application of the same filter for all the frequency/scale components of the signal. However, the rich spectral content of the seismic signals makes more desirable to be able to adapt the filter at each frequency/scale.

In the proposed approach, we decompose each seismic trace in a time-scale-slowness domain to increase the signal-to-noise ratio and the seismic event tracking capability w.r.t. an adaptive LSST approach, while keeping the time resolution. The high degree of freedom that the time-scale domain provides enables the design of a large set of filters much more selective in slowness that the equivalent LSST ones. This freedom allows us to set the optimum slowness resolution at each frequency, or in opposition, to keep the resolution constant to build filters that preserve the waveform of the seismic signals processed. Additionally, it is also possible to configure these filters to mimic a large variety of slowness filters in the *f-k*, *p-f* and τ-p domain, reducing problems of aliasing in the first ones and of inversion in the last ones.

2.1 Analysis

The local time-scale slant-stack transform is a combination of the LSST and a continuous wavelet transform. The LSST of a seismic section u with a nonuniform separation between traces can be written as a weighted sum of L neighboring traces along a set of signal trajectories of slope/slowness p_s, being s the slope/slowness index:

$$v_{s,m}[n] = \sum_{l=-(L-1)/2}^{(L-1)/2} g_m[l]\, u_{m+l}(nT + (d_{m+l} - d_m)\, p_s)$$

where each element $v_{s,m}[n]$ of the LSST decomposition is an estimation of the contribution of the signal s to the sample $u_m(nT)$, being n and m the sample and trace indices, respectively. The time-space trajectory of the wavefront with a slowness p_s is $t = nT + (d_{m+i} - d_m)p_s$, where T is the sampling period and $d_{m+i} - d_m$ the distance between the traces u_m and u_{m+i}. The space window $g_m[l]$ is a smooth unit area function that may depend on the offset of u_m. And L may change along any dimension.

The equivalent time-scale LSST operation can be written as the above LSST but performed in a time-scale domain:

$$Wv_{s,m}[n,j] = \sum_{l=-(L-1)/2}^{(L-1)/2} g_\lambda[l]\, Wu_{m+l}(nT + (d_{m+l} - d_m)\, p_s, 2^j)$$

where $Wu_m(\tau,\lambda)$ stands for the wavelet transform along time in the seismic section $u(t,x)$. Each element $Wv_{s,m}[n,j]$ is the contribution at scale $\lambda = 2^j$ of the signal s at the sample n of the trace with offset $x = d_m$.

For a proper performance of the above slowness decomposition, the wavelet transform and its inverse have to fulfill three essential features: nearly perfect reconstruction, to reduce estimation errors on the slowness components of the signal; linear phase delay, to preserve the seismic waveform; and close-to time-invariance, to reduce the interpolation error at required time-scale positions not provided by the discretized wavelet transform. Additionally, it is useful to have freedom in the choice of the mother wavelet. For this reason, we have chosen an oversampled complex wavelet transform based on frames of wavelets with several voices per octave.

2.2 Filtering and synthesis

A seismic section decomposed in time, space, scale and slowness that contains R coherent signals of q_r slowness, $u_r(t - q_r x)$ with $r \in [1,R]$, can be approximately modeled as:

$$Wv_{s,x_c}(\tau,\lambda) \simeq \sum_{r=1}^{R} h(\lambda, q_r - p_s)\, Wu_r(\tau - q_r x_c, \lambda) \qquad (1)$$

where $h(\lambda, q_r - p_s)$ denotes a transfer function that models the cross-interference in the slowness axis and x_c the offset of a given trace.

This transfer function depends on the LSST space window $g(x)$ and the mother wavelet $\psi(t)$,

$$h(\lambda, q_r - p_s) = \frac{1}{\lambda^2 C_\psi} \int_{-\infty}^{\infty} \psi_\lambda(\tau)\, \psi^*_{1_\lambda}(\tau, q_r - p_s)\, d\tau \qquad (2)$$

where $C_\psi = \int_{-\infty}^{\infty} |\hat{\psi}(\omega)|^2/|\omega| d\omega$ and $\psi_{1_{\lambda,s}}(t)$ denotes the family of functions used in the time-scale LSST,

$$\psi_{1_\lambda}(\tau, q_r - p_s) = \int_{-\infty}^{\infty} \frac{1}{|q_r - p_s|}\, g_\lambda\left(\frac{t}{q_r - p_s}\right) \psi_\lambda(t - \tau) dt$$

Note that $g(t)$ is smooth, has unit area and is positive around zero. In this work, we synthesized the filtered section using a conventional 1D inverse continuous wavelet transform, but other options are possible, such as a unique family of functions for analysis and synthesis, similarly to the approach of curvelet frames [15].

The optimum scaling of $g(x)$ is problem dependent, and generally not linear with the scale. As a consequence, $\psi_{1_{\lambda,s}}(t)$ cannot be obtained by scaling and translating a

unique mother wavelet; except in the particular case where the window length is proportional with the scale, in which case the transfer function is scale independent,

$$h(q_r - p_s) = \frac{1}{C_\psi} \int_0^\infty \hat{g}((q_r - p_s)\,\omega)\,|\hat{\psi}(\omega)|^2\,\frac{d\omega}{\omega} \qquad (3)$$

and (1) is exact. In (3), $\hat{\psi}(\omega)$ and $\hat{g}(\omega)$ denotes the Fourier transform of the mother wavelet and the space window, respectively. A filtered seismic section in the time-scale LSST domain can be written using the transfer function defined in (2) as:

$$Wy_{x_c}(\tau,\lambda) = \sum_{s=1}^{S}\sum_{r=1}^{R} f(\tau,\lambda,p_s)h(\lambda,q_r-p_s)Wu_r(\tau - q_r x_c,\lambda) \qquad (4)$$

where $Wy_{x_c}(\tau,\lambda)$ denotes the filtered signal in the time-space-scale domain and $f(\tau,\lambda,p_s)$ the weighting filter to design.

If we define $k_r(\tau,\lambda)$ as the desired gain for the r slowness, the filter to design has to satisfy R equations. From (4),

$$\sum_{s=1}^{S} f(\tau,\lambda,p_s)h(\lambda,q_r-p_s) = k_r(\tau,\lambda) \quad r \in [1,R]$$

or in vector notation,

$$\mathbf{H}(\lambda)\mathbf{f}(\tau,\lambda) = \mathbf{k}(\tau,\lambda) \qquad (5)$$

This system of equations is underdetermined, $S \gg R$, and it thus possesses an infinite number of solutions. When the instantaneous slowness of each coherent signal is known, the least-squares solution leads to the minimum noise level in the slowness axis. Considering a white Gaussian noise, the solution of (5) under the minimum L^2 norm constraint:

$$\min_{\mathbf{f}(\tau,\lambda)} \mathbf{f}^T(\tau,\lambda)\mathbf{f}(\tau,\lambda) \quad \text{that} \quad \mathbf{H}(\lambda)\mathbf{f}(\tau,\lambda) = \mathbf{k}(\tau,\lambda)$$

is

$$\mathbf{f}(\tau,\lambda) = \mathbf{H}(\lambda)\left(\mathbf{H}^T(\lambda)\mathbf{H}(\lambda)\right)^{-1}\mathbf{k}(\tau,\lambda)$$

To design this 4D filter it is necessary to set $k_r(\tau,\lambda)$ appropriately. In order to design this filter automatically, we estimated the local maxima of the modulus of the complex time-scale LSST through instantaneous slowness measures of the most coherent signals in the slowness range of interest.

3. M-BAND WAVELETS AND HILBERT PAIRS

Let M be an integer greater than or equal to 2. An M-band multiresolution analysis of $\mathbb{L}^2(\mathbb{R})$ is defined by one scaling function $\psi_0 \in \mathbb{L}^2(\mathbb{R})$ and $(M-1)$ mother wavelets $\psi_m \in \mathbb{L}^2(\mathbb{R})$, $m \in \{1,\ldots,M-1\}$ [19], solutions of the following scaling equations:

$$\forall m \in \{0,\ldots,M-1\}, \quad \frac{1}{\sqrt{M}}\psi_m\Big(\frac{t}{M}\Big) = \sum_{k=-\infty}^{\infty} h_m[k]\,\psi_0(t-k), \qquad (6)$$

where the sequences $(h_m[k])_{k\in\mathbb{Z}}$ are square integrable. A "dual" M-band multiresolution analysis is defined by a scaling function ψ_0^{H} and mother wavelets ψ_m^{H}, $m \in \{1,\ldots,M-1\}$

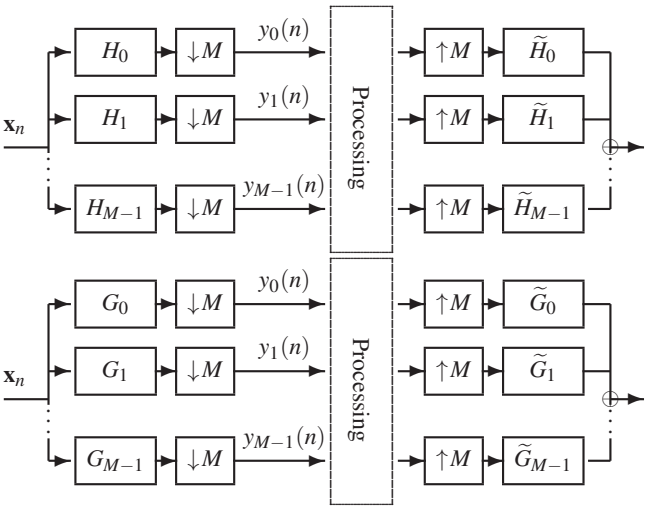

Figure 2: A pair of analysis/synthesis M-band para-unitary filter banks generating M-band dual-tree wavelets.

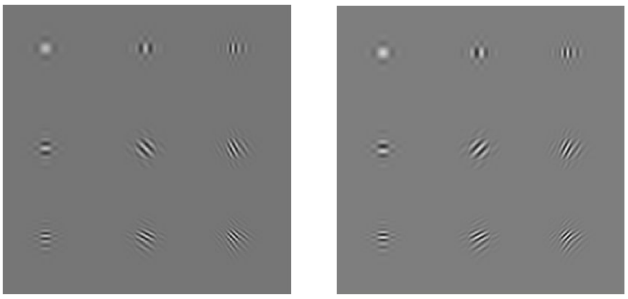

Figure 3: Bidimensional 3-band dual-tree wavelets: (Left) negatively oriented scaling function and wavelets; (Right) positively oriented counterparts.

related to the functions ψ_m by an Hilbert pair relationship. More precisely, the dual mother wavelets will be obtained by an Hilbert transform from the "primal" wavelets ψ_m, $m \in \{1,\ldots,M-1\}$. In the Fourier domain, the Hilbert transform reads:

$$\forall m \in \{1,\ldots,M-1\}, \qquad \widehat{\psi}_m^{\mathrm{H}}(\omega) = -\imath\,\mathrm{sign}(\omega)\,\widehat{\psi}_m(\omega).$$

where the signum function sign is defined as:

$$\mathrm{sign}(\omega) = \begin{cases} 1 & \text{if } \omega > 0 \\ 0 & \text{if } \omega = 0 \\ -1 & \text{if } \omega < 0. \end{cases}$$

These dual wavelets also satisfy two-scale equations similar to (6) with the square integrable sequences $(g_m[k])_{k\in\mathbb{Z}}$. The general representation in terms of filter banks, on one decomposition level, is shown in Fig. 2. Two-dimensional extensions are obtained by tensor product between primal and dual wavelets and linear combinations [3], as represented in Fig. 3 with $M = 3$ bands.

They illustrate that different directions can be extracted from the transform, since band- and high-pass wavelets select opposite directions for each tree. Since the present paper focuses on applications, we refer to [17, 4] for further

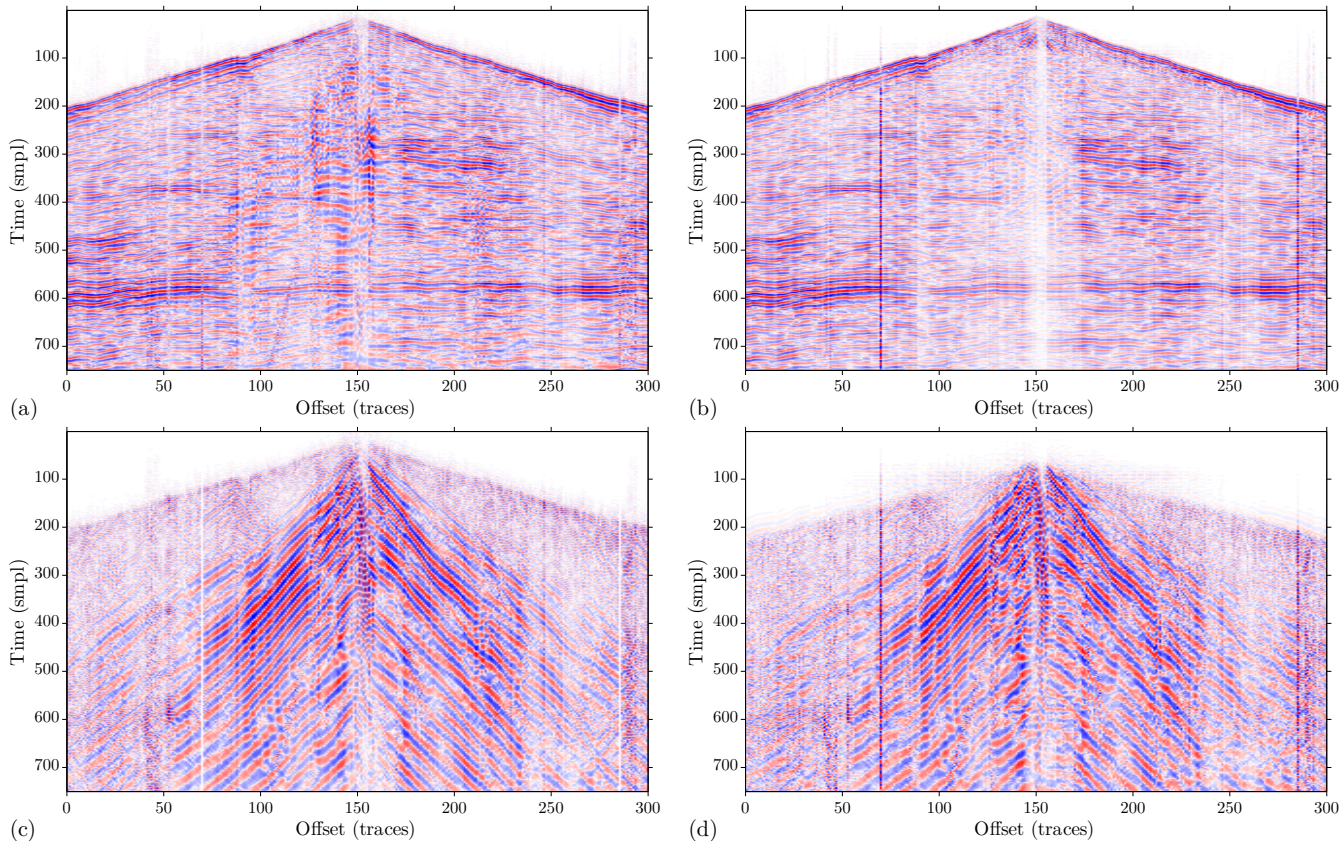

Figure 4: Filtered signal (a) using the time-scale LSST to remove the high slope interferent signals, and (b) with local mute of dual-tree coefficients, together with their differences w.r.t. original data in (c) and (d).

details on dual-tree wavelet transforms. In contrast to traditional wavelet shrinkage where small coefficients are discarded, high-valued coefficients are masked since they correspond to aforementioned coherent noises [9].

4. RESULTS AND DISCUSSION

To compare the two approaches, they are applied to coherent noise removal from dataset in Fig. 1. It represents 750×300 seismic image acquired in a rugged tomography foothill province. The occluding coherent noise under consideration is located at the acute cone originating from the central apex. Its highly energetic and directional characteristics, since it does not bear significant information, prevents the estimation of geological substructures with lower amplitude.

To better qualify the filters' behavior and results, the Structural Similarity Index (SSIM) [23], now commonly employed for image quality assessment, has been applied. The SSIM was initially proposed to overcome the limitations of standard metrics used in image comparison and evaluation such as mean squared error or peak signal-to-noise ratio. Although the nature of seismic data is rather specific and differs from natural images, computing similarity maps (Fig. 5) between the original data and filtered estimations provides meaningful insights. Local high SSIM measures between original and filtered data correspond to close shape.

Most of the differences between the results obtained with both filtering techniques, apparent on Figs. 4 and 5, are related to their different space-slowness trade-off. Both techniques attenuate the main high-slope coherent-noise components (mid part on all these figures) with a higher attenuation in the case of the dual-tree based filter — high SSIM value — thanks to its shorter filter response or equivalently higher space resolution w.r.t. the other. However, due to its lower slowness resolution the distortion on low-slope signals are higher. This effect can be noticed on the higher SSIM measures on the outer part of Fig. 5(b), while the measures of Fig. 5(a) are lower since the time-scale LSST based filter gives a higher slowness resolution in accordance with its longer filter response. High-resolution figures are made available at [21].

5. CONCLUSIONS

Time-scale directional filters are a powerful tool that can significantly improve seismic data processing, thanks to the enhancement in the seismic wave detection, separation and tracking capabilities. The flexibility of these tools enables adaptive instantaneous slowness with a fair degree of control of the slowness resolution in time-scale, while keeping a minimum level of distortion to the signals under analysis. As interferences are processed at each trace in the time-scale-slowness domain, it becomes possible to isolate them, in contrast to the commonly used τ-p transform and f-k pie-slice based filters because of the lack of space resolution of the former and of time-space resolution of the latter. The two techniques used in this context yield two complementary approaches, with a different balance in slowness reso-

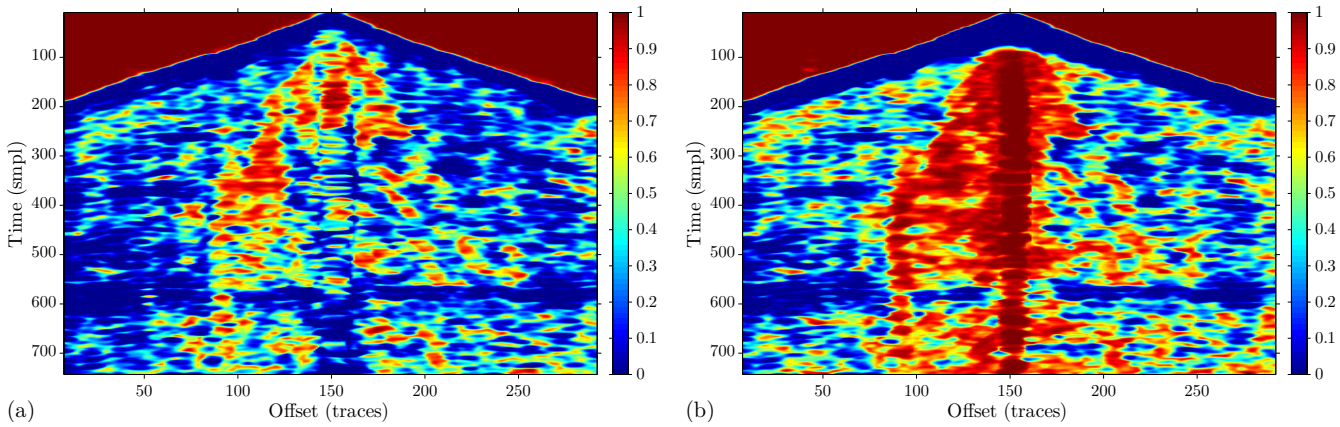

Figure 5: Similarity maps between original data and estimated interferent signals using (a) the time-scale LSST, and (b) the dual-tree wavelets.

lution and redundancy. Both are able to attenuate the main part of the chevron-like coherent noise occluding meaningful geologic information. The time-scale LSST focuses on a reduced distortion level of the signal of interest, while the dual-tree wavelet transform aims at increased noise rejection. Due to the similarity of the time-scale LSST with other directional transforms used in image processing [1, 15], the quest for a vaster family of adaptive transforms linking proposed methods deserves further investigations.

6. ACKNOWLEGDEMENTS

The local adaptive slant stack filters in the time-scale domain have their origin in the Ph.D. thesis of Sergi Ventosa at the UTM-CSIC supervised by Carine Simon, Martin Schimmel and Juanjo Dañobeitia.

References

[1] S. Berlemont, A. Bensimon, and J.-C. Olivo-Marin. Feature-adapted fast slant stack. In *Proc. Int. Conf. Image Process.*, volume 4, pages 57–60, Oct. 2007.

[2] T. Bohlen, S. Kugler, G. Klein, and F. Theilen. 1.5D inversion of lateral variation of Scholte-wave dispersion. *Geophysics*, 69(2):330–344, 2004.

[3] C. Chaux, L. Duval, and J.-C. Pesquet. Image analysis using a dual-tree M-band wavelet transform. *IEEE Trans. Image Process.*, 15(8):2397–2412, Aug. 2006.

[4] C. Chaux, J.-C. Pesquet, and L. Duval. Noise covariance properties in dual-tree wavelet decompositions. *IEEE Trans. Inform. Theory*, 53(12):4680–4700, Dec. 2007.

[5] J. Claerbout. *Fundamentals of geophysical data processing with applications to petroleum prospecting*. Blackwell Scientific Publications, 1985. Available at http://sepwww.stanford.edu/sep/prof/.

[6] A. Dev and G. A. McMechan. Spatial antialias filtering in the slowness-frequency domain. *Geophysics*, 74(2):V35–V42, 2009.

[7] H. Douma and M. V. de Hoop. Leading-order seismic imaging using curvelets. *Geophysics*, 72(6):S231–S248, 2007.

[8] T. Durrani and D. Bisset. The Radon transform and its properties. *Geophysics*, 49(8):1180–1187, 1984.

[9] L. Duval, C. Chaux, and S. Ker. Coherent noise removal in seismic data with dual-tree M-band wavelets. In *Proc. SPIE, Wavelets: Appl. Signal Image Process.*, San Diego, CA, USA, Aug. 2007.

[10] P. Flandrin. *Time-frequency and time-scale analysis*. Academic Press, San Diego, USA, 1998.

[11] T. Forbriger. Inversion of shallow-seismic wavefields: I. wavefield transformation. *Geophysical Journal International*, 153(3):719–734, 2003.

[12] W. S. Harlan, J. F. Claerbout, and F. Rocca. Signal/noise separation and velocity estimation. *Geophysics*, 49(11):1869–1880, 1984.

[13] G. Hennenfent and F. J. Herrmann. Seismic denoising with nonuniformly sampled curvelets. *Computing in Science & Engineering*, 8(3):16–25, 2006.

[14] L. Jacques, L. Duval, C. Chaux, and G. Peyré. A panorama on multiscale geometric representations, intertwining spatial, directional and frequency selectivity. *Signal Process.*, 2011. In press.

[15] J. Ma and G. Plonka. The curvelet transform — a review of recent applications. *IEEE Signal Process. Mag.*, 27(2):118–133, Mar. 2010.

[16] E. Magli, G. Olmo, and L. L. Presti. Pattern recognition by means of the Radon transform and the continuous wavelet transform. *Signal Process.*, 73(3):277–289, 1999.

[17] I. W. Selesnick, R. G. Baraniuk, and N. G. Kingsbury. The dual-tree complex wavelet transform. *IEEE Signal Process. Mag.*, 22(6):123–151, Nov. 2005.

[18] A. Shlivinski, E. Heyman, and A. Boag. A pulsed beam summation formulation for short pulse radiation based on windowed Radon transform (WRT) frames. *IEEE Trans. Antenn. Propag.*, 53(9):3030–3048, 2005.

[19] P. Steffen, P. N. Heller, R. A. Gopinath, and C. S. Burrus. Theory of regular M-band wavelet bases. *IEEE Trans. Signal Process.*, 41(12):3497–3511, Dec. 1993.

[20] P. L. Stoffa, P. Buhl, J. B. Diebold, and F. Wenzel. Direct mapping of seismic data to the domain of intercept time and ray parameter–a plane-wave decomposition. *Geophysics*, 46(3):255–267, 1981.

[21] S. Ventosa. Addendum. http://www.laurent-duval.eu/ventosa-2011-eusipco-lsst.html.

[22] V. D. Vrabie, N. L. Bihan, and J. I. Mars. Multicomponent wave separation using HOSVD/unimodal-ICA subspace method. *Geophysics*, 71(5):V133–V143, 2006.

[23] Z. Wang and Q. Li. Information content weighting for perceptual image quality assessment. *IEEE Trans. Image Process.*, (99), 2011. Accepted, in print.

[24] Ö. Yilmaz. *Seismic data analysis: processing, inversion, and interpretation of seismic data*. Soc. Expl. Geophysicists, 2001.